Journal of Power Sources 239 (2013) 196–200

Contents lists available at SciVerse ScienceDirect

Journal of Power Sources

journal homepage: www.elsevier.com/locate/jpowsour

Short communication

Electrochemical characterization of $La_{0.6}Ca_{0.4}Fe_{0.8}Ni_{0.2}O_{3-\delta}$ perovskite cathode for IT-SOFC

N. Ortiz-Vitoriano [a], A. Hauch [b], I. Ruiz de Larramendi [a], C. Bernuy-López [b,c], R. Knibbe [b,1], T. Rojo [a,c,*]

[a] Departamento de Química Inorgánica, Facultad de Ciencia y Tecnología, Universidad del País Vasco UPV/EHU, Apdo. 644, 48080 Bilbao, Spain
[b] DTU Energy Conversion and Storage, Technical University of Denmark, Frederiksborgvej 399, DK-4000 Roskilde, Denmark
[c] CIC energiGUNE, Parque Tecnológico de Álava, Albert Einstein 48, 0150 Miñano, Spain

HIGHLIGHTS

- $La_{0.6}Ca_{0.4}Fe_{0.8}Ni_{0.2}O_3$ electrodes were studied by impedance spectroscopy.
- The electrodes were produced at a range of different sintering temperatures.
- An equivalent circuit was constructed to describe the polarization losses.
- Cell sintered at 750 °C exhibits favorable oxygen reduction reaction properties.

ARTICLE INFO

Article history:
Received 8 January 2013
Received in revised form
5 March 2013
Accepted 24 March 2013
Available online 2 April 2013

Keywords:
Solid oxide fuel cell
Cathode
Electrochemical impedance spectroscopy
Mixed conductors

ABSTRACT

Electrolyte supported symmetric cells featuring $La_{0.6}Ca_{0.4}Fe_{0.8}Ni_{0.2}O_3$ (LCFN) electrodes are studied by electrochemical impedance spectroscopy. The aim is to describe the polarization losses of this mixed ionic electronic conductor electrode at various cell operating conditions for cells sintered at different temperatures. An equivalent circuit describing the cathode polarization resistances was constructed from analyzing impedance spectra recorded at different oxygen partial pressures and temperatures. Favorable oxygen reduction reaction properties are demonstrated for the LCFN cell sintered at 750 °C with a polarization resistance of 0.05 Ω cm^2 at an operating temperature of 800 °C in pure oxygen.

1. Introduction

Solid oxide fuel cells (SOFC) are electrochemical devices which convert chemical energy directly into electrical energy with high efficiency and low environmental impact [1]. In order to limit cathode overpotential the traditional SOFC, with an yttria-stabilized zirconia (YSZ) electrolyte and a strontium-doped lanthanum manganite (LSM) cathode, typically operates at relatively high temperatures (800–1000 °C). These high temperatures increase balance of plant costs and encourage certain types of cell degradation [2] – making a lower operating temperature (600–800 °C) desirable. Cells which operate in this lower temperature range are known as intermediate temperature SOFCs (IT-SOFC). In order to operate at IT-SOFC temperatures, new cathode materials are required and the processing routes must be optimized. SOFC materials development also requires further insight into the mechanisms responsible for the overpotential losses in the cathode material, for which Electrochemical Impedance Spectroscopy (EIS) is a powerful investigative tool.

In this work, electrolyte supported symmetrical cells featuring $La_{0.6}Ca_{0.4}Fe_{0.8}Ni_{0.2}O_3$ (LCFN) electrodes were produced as previously described at a range of different sintering temperatures (T_s) [3]. The symmetric cell configuration was chosen to study the cathode processes as the data interpretation is simpler compared to a full SOFC analysis. To determine the resistance of the various cathode processes, the manufactured cells were characterized by EIS between 600 and 800 °C and at several oxygen partial pressures (pO_2). In addition to complex non-linear least squares (CNLS) fitting

* Corresponding author. Departamento de Química Inorgánica, Facultad de Ciencia y Tecnología, Universidad del País Vasco UPV/EHU, Apdo. 644, 48080 Bilbao, Spain. Tel.: +34 94 6012458; fax: +34 94 6013500.
E-mail address: teo.rojo@ehu.es (T. Rojo).
[1] Present address: Industrial Research Limited, Wellington 5040, New Zealand.

0378-7753/$ – see front matter © 2013 Elsevier B.V. All rights reserved.
http://dx.doi.org/10.1016/j.jpowsour.2013.03.121

of the impedance spectra (IS), the distribution of relaxation time (DRT) of the IS was investigated to provide a model-independent insight into the cathode processes [4].

2. Experimental

2.1. Cell specifications

The cells used for the electrochemical testing in this study are electrolyte supported symmetric cells produced at the Technical University of Denmark (DTU). LCFN was prepared by the liquid mix method described elsewhere [5]. The cell consists of a 200 μm thick, dense, 8 mol% Y_2O_3 stabilized ZrO_2 (YSZ) electrolyte produced via tape-casting, sandwiched between two LCFN electrodes, each deposited by a spray casting technique. A series of symmetric cells were produced sintered from 750 to 1000 °C, at increments of 50 °C. The shorthand notation of *T*-cell will be used throughout, where *T* represents the T_s of the symmetric cells. Details of the cathodes' structural properties and the cells' microstructure are given elsewhere [3].

2.2. Cell test set-up

The cell dimensions were 5.0 × 5.0 mm^2. Pt-paste was applied onto the electrode surfaces for current collection. The test rig used for the experiments had four sample positions. At least two identical symmetrical cells were placed in the set-up and measured simultaneously in order to check reproducibility.

2.3. Electrochemical impedance spectroscopy

EIS was measured at open circuit voltage (OCV) with a Solartron 1260 Frequency Response Analyzer between 600 and 800 °C, in the frequency range 10^6–0.05 Hz with 12 points/decade. IS were recorded at three different pO_2 (0.2, 0.5 and 1 atm) for the 750-cell and at 1 atm for all other cells. The desired pO_2 was obtained by mixing O_2 and N_2. IS were analyzed using Scribner Associates' Zview software.

2.4. Morphological characterization – post-test analysis

Polished cross sections of the symmetrical cells after electrochemical tests were investigated by scanning electron microscopy (SEM) using a Zeiss Cross-beam 1540XB equipped with a field-emission gun.

3. Results and discussion

3.1. Qualitative analysis of impedance spectra – equivalent circuit model development

The 750-cell was chosen to develop the equivalent circuit for the LCFN/YSZ/LCFN symmetric cell. IS were recorded at different temperatures and pO_2. The data was first analyzed in terms of DRT with the peak shapes and features providing information on the nature of the contributing processes.

Fig. 1 shows DRT spectra obtained at three different pO_2 for the 750-cell at 650 °C. In all the DRT spectra two peaks are observed – one symmetrical peak at high frequencies ($f_{peak} \sim 10^5$ Hz) and one asymmetrical peak at lower frequencies ($f_{peak} \sim$ 70–270 Hz). The high frequency peak is weakly pO_2 dependent and can be described well by a parallel RQ-element. The summit frequency for the lower frequency peak shifts to higher frequencies with increasing pO_2. The contribution of this peak is more complex but can be well described by an RQ-element and a Gerischer element in series. An

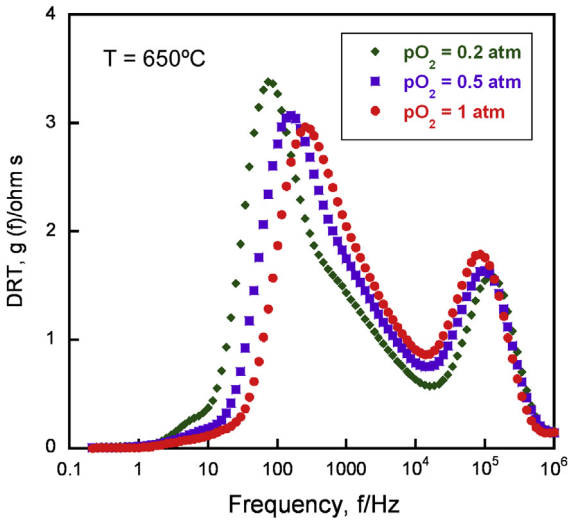

Fig. 1. DRT spectra obtained from IS obtained on the 750-cell at a pO_2 of 0.2, 0.5 and 1 atm at 650 °C.

additional peak is observed in the $pO_2 = 0.2$ atm spectra at very low frequencies (<10 Hz), but is completely absent in the 1 atm spectra. This process is assigned to oxygen gas diffusion and has not been included in the equivalent circuit modeling due to its small/negligible contribution to R_p. These results are in good agreement with the kinetics of porous mixed-conducting oxygen electrodes described by Adler et al. [6]. The resulting equivalent circuit from the DRT analysis is L–Rs–RQ_1–RQ_2–G. The values, presented in the following section, are from CNLS fitting the IS with this equivalent circuit. The applied model is in good agreement with those reported in literature for similar cathode materials [7,8].

3.2. Quantitative analysis of impedance spectra – CNLS fitting

Fig. 2 shows the DRT and IS at $pO_2 = 1$ atm, recorded at 600, 650 and 700 °C together with CNLS fit results. The individual R_p circuit element responses, from the L–Rs–RQ_1–RQ_2–G model, are included in Fig. 2(b–d). This shows that the R_p response described by the Gerisher element is found at the lowest frequencies. Similar fits were obtained for the other symmetrical cells.

Fig. 2a shows that the DRT peaks shift toward high frequencies with increasing temperature. Furthermore, the intermediate to low frequency range features dominate the R_p. Table 1 summarizes the main CNLS fit results and calculated activation energies for each process. The R_p value trends (Table 1) correspond well with the qualitative observations made for Fig. 2 i.e. 1) the R_p decreases with increasing temperature and 2) the intermediate and low frequency R_p contributions dominate the cells' resistance. The R_p circuit elements' activation energies are 1.15, 1.60 and 1.88 eV for the high, intermediate and low processes, respectively. Fig. 3 identifies, schematically, the location of these electrode processes according to the fitting.

The high frequency process ($E_a = 1.15$ eV; $f_{summit} \sim 100$ kHz at 650 °C) is independent of pO_2, and has an E_a similar to the E_a for oxide ion migration at grain boundaries in YSZ electrolyte (1 eV) [9]. This process is assigned to oxygen ion transfer from the MIEC to oxygen vacancies in the electrolyte (Fig. 3e) [13].

In contrast to the high frequency arc, the lower frequency arcs are pO_2 sensitive. The arc observed at intermediate frequency ($E_a = 1.6$ eV; $f_{summit} = 1500$ Hz at 650 °C, RQ_2) and low frequency ($E_a = 1.88$ eV; $f_{summit} = 559$ Hz at 650 °C, Gerischer) are assigned to the dissociative adsorption of O_2 (Fig. 3a & b) followed by

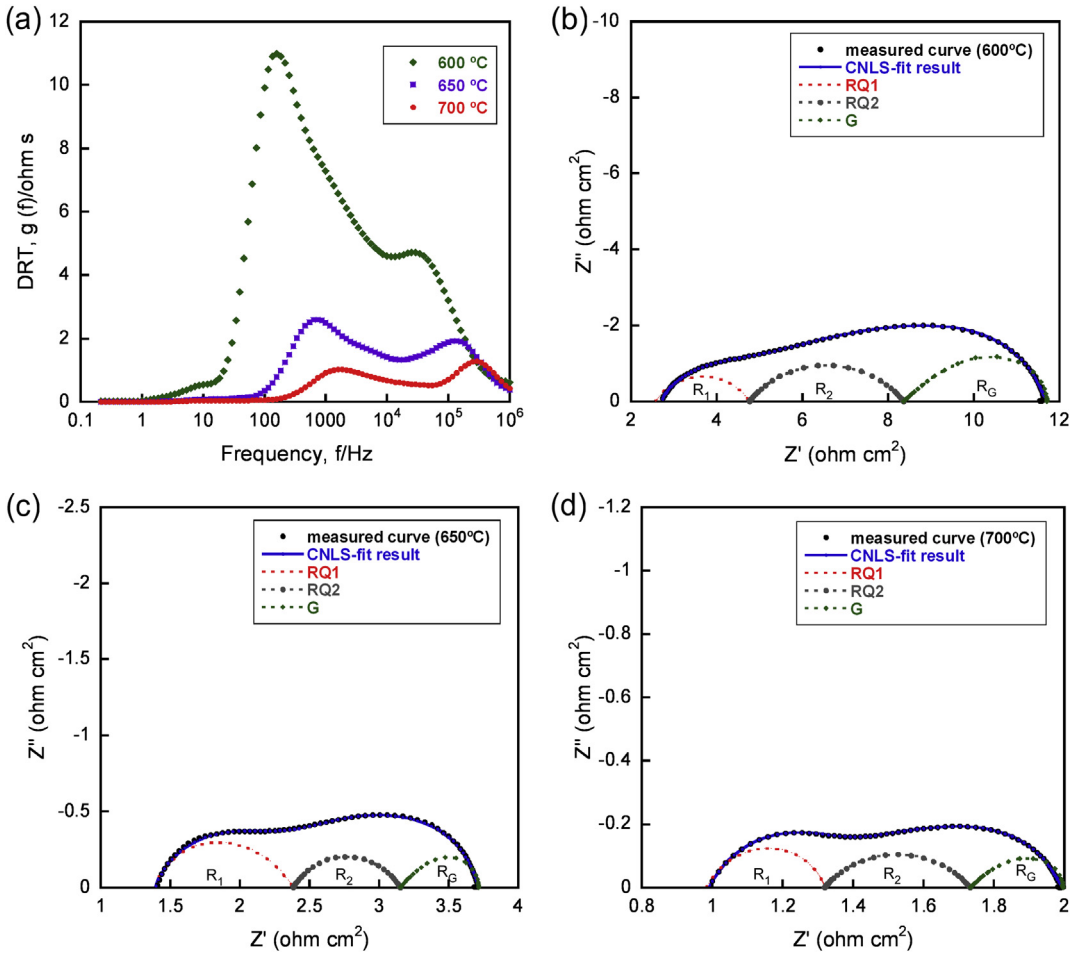

Fig. 2. DRT spectra at 600, 650 and 700 °C for the 750-cell at $pO_2 = 1$ atm (a) and IS and corresponding CNLS fit results for IS recorded at 600 °C (b), 650 °C (c) and 700 °C (d). Dotted lines in (b), (c) and (d) represent the individual elements (RQ_1–RQ_2–Gerischer) in the CNLS fit.

electrochemical reduction (Fig. 3c) and transfer of oxygen species to the electrode–electrolyte interface (Fig. 3d) [6,14]. More specifically, the intermediate frequency process is ascribed to dissociative adsorption, transfer of species at the TPB and surface diffusion [10] and the low frequency contribution reflects competitive elementary processes in the electrochemical reduction mechanism (Fig. 3c) [11]. This low frequency process had been suggested to limit the performance of both the LCFN and $La_{0.6}Ca_{0.4}MnO_3$ cathodes based on the activation energy, pO_2 dependence and the characteristic frequency observed [12]. The Gerischer impedance is applied to describe MIEC electrode responses in systems where an electrochemical reaction is coupled to an oxide ion diffusion process along different pathways i.e. through the bulk, at the surface or a combination of both. This element suggests that bond breaking and surface diffusion maybe rate limiting for the electrochemical reduction process [15].

Table 1
Summary of CNLS fitting results of inductance corrected IS recorded at $pO_2 = 1$ atm for the 750-cell at 600 °C, 650 °C and 700 °C. Also included are the calculated activation energies (E_a) for each process. Resistances (R) in Ω cm^2, characteristic frequencies (f) in Hz.

	600 °C	650 °C	700 °C	E_a (eV)
R_S	2.57	1.20	0.87	1.27
R_1	2.19	1.18	0.45	1.15
f_1	33000	100000	300000	
R_2	3.606	0.77	0.41	1.60
f_2	760	1500	5300	
R_G	3.34	0.56	0.26	1.88
f	150	559	1510	

3.3. Electrode microstructure after electrochemical tests

Fig. 4 shows the SEM images of cross-sections of the LCFN/YSZ/LCFN symmetrical cells sintered at 800, 900 and 1000 °C after electrochemical testing. The 750-cell shows no discernible difference from that sintered at 800 °C. SEM analysis prior to testing is reported in our previous publication [3]. LCFN grain size and electrode density both increase with T_s. This is accompanied by a significant reduction of LCFN porosity which reduces the LCFN-surface/gas interface. Additionally, $CaZrO_3$ formation is observed at the cathode/electrolyte interface from 850 up to 1000 °C. The $CaZrO_3$ layer thickness increases with T_s, with only the 1000-cell exhibiting noticeable change post-electrochemical testing (increasing from 400 to 600 nm). SEM investigations therefore reveal little change in LCFN grain size, interaction layer or electrode density as a result of electrochemical testing, indicating no detrimental effects.

3.4. Effect of sintering temperature on the electrochemical performance

Table 2 summarizes the R_p and R_s for the 750-cell, 800-cell and 1000-cell. The 750-cell, first reported in the present work, has the smallest R_p of all the tested symmetrical cells with an R_p of

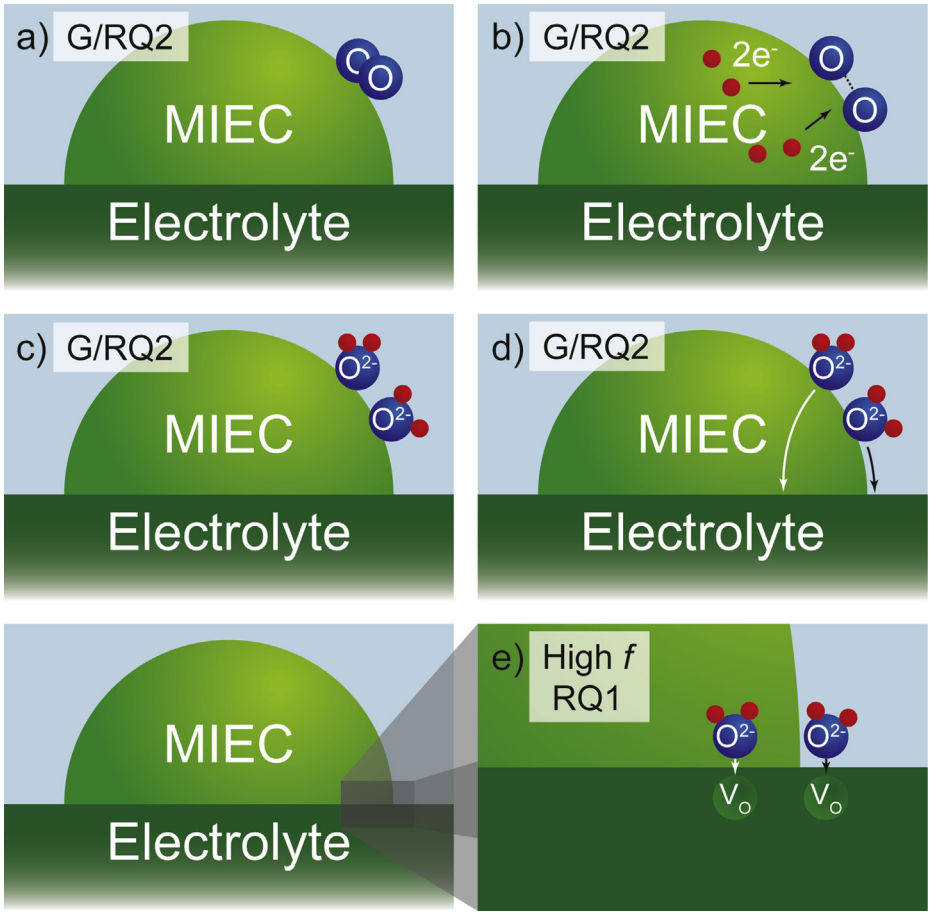

Fig. 3. Schematic of the proposed LCFN electrode processes. a) O_2 adsorption, b) O dissociation; c) electrochemical reduction to O^{2-}; d) O^{2-} migration to electrode/electrolyte interface and e) incorporation into O vacancies in YSZ electrolyte.

0.05 Ω cm^2 at 800 °C and a pO_2 of 1 atm. Increasing T_s increases R_p. The R_p of the 750-cell shows a marked improvement of 60% compared to that of the 800-cell. The R_p values are comparable with those obtained for the high-performing (La,Sr)(Fe,Co)O_3 cathode [16]. Increasing the T_s increases the R_p, due to 1) the formation of an insulating $CaZrO_3$ phase at the electrode/electrolyte interface and 2) the loss of electrode porosity [3]. As the $CaZrO_3$ insulating layer is comparatively thin (ca. 400 nm for 1000-cell prior to testing) with respect to the electrolyte thickness (200 μm), the R_s is not significantly affected within the T_s range investigated (800–1000 °C). The LCFN/YSZ/LCFN symmetric cells sintered at low temperatures (750, 800 °C) show the smallest grain size and most open porosity, thus resulting in large LCFN surface area and lower R_p values.

To the best of our knowledge, this is the first time a symmetric cell for SOFC application has been sintered at such low temperature (750 °C), which provides new possibilities for a more economical production route. Furthermore, a cathode T_s of only 750 °C is highly relevant for metal-supported SOFCs and in general for SOFCs where nano-sized particles are impregnated for increased catalytic activity [17]. The LCFN cathode performance is better than the state-of-the-art (La,Sr)(Fe,Co)O_3 on $Y_{0.08}Zr_{0.92}O_{1.96}$/$Gd_{0.1}Ce_{0.9}O_2$ electrolyte with a R_p value of 0.142 Ω cm^2 in air at 850 °C when sintered at 1400 °C [18] and better than $LaSrMnO_3$ on YSZ electrolyte with a R_p value of 9 Ω cm^2 in air at 700 °C when sintered at 1250 °C (this work: 0.56 Ω cm^2 for the 750-cell) [19]. Similar values have been obtained for the LSM/YSZ composite at 850 °C with R_p values of 0.115 Ω cm^2 in oxygen [14]. The development of the equivalent

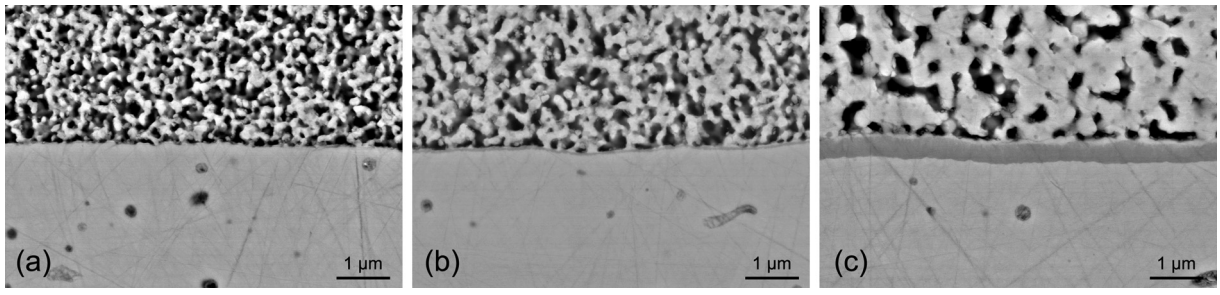

Fig. 4. SEM images of the cross section of LCFN/YSZ/LCFN symmetric cells after electrochemical tests: (a) 800-cell, (b) 900-cell and (c) 1000-cell.

Table 2
R_s and R_p obtained from CNLS fitting IS on the 750-cell, 800-cell and 1000-cell at temperatures from 600 °C to 850 °C. Resistances are given in Ω cm^2. Measured at $pO_2 = 1$ atm.

Characterization temperature (°C)	750-Cell		800-Cell		1000-Cell	
	R_s	R_p	R_s	R_p	R_s	R_p
600	2.57	4.56	4.18	4.25	3.96	2444
650	1.2	1.25	2.25	1.99	2.95	1266
700	0.87	0.56	1.32	0.72	1.68	407
750	0.57	0.16	0.85	0.23	1.07	125
800	0.41	0.05	0.61	0.08	0.58	42

circuit model increases the understanding of the nature of the processes involved and can be taken as a first indication that the oxygen surface exchange and/or partial ionic conductivity influence the LCFN electrode performance.

4. Conclusions

$La_{0.6}Ca_{0.4}Fe_{0.8}Ni_{0.2}O_3$ material has been developed as an intermediate temperature solid oxide fuel cell cathode material with excellent electrochemical performance. Symmetric cells were fabricated using yttria-stabilized zirconia as the electrolyte. An equivalent circuit model was developed for analysis of impedance spectra and used for characterization of the individual polarization losses observed. This was achieved by CNLS fitting and analysis of DRT for impedance spectra from 600 to 800 °C in pO_2 from 0.2 to 1 atm. To describe the processes in the cathode an equivalent circuit models described by L–Rs–RQ_1–RQ_2–G was applied. The 750-cell reveals a high electrochemical performance with an R_p of 0.05 Ω cm^2 at 800 °C.

Acknowledgments

This work has been partially financed by the Spanish CiCyT under project MAT2010-19442 and by the Government of the Basque Country under project IT-312-07, SAIOTEK S-PE11UN064 and S-PE12UN140. N. Ortiz-Vitoriano thanks the University of the Basque Country (UPV/EHU) for funding her research activities under the "Especialización de Personal Investigador del Vicerrectorado de Investigación de la UPV/EHU" programme and Dr. Stuart Cook for fruitful discussions. The basic funded project "SOECells" supported the part of this work that was undertaken at DTU Energy Conversion and Storage, Risø Campus, Technical University of Denmark.

References

[1] B.C.H. Steele, A. Heinzel, Nature 414 (2001) 345–352.
[2] R. Knibbe, A. Hauch, J. Hjelm, S.D. Ebbesen, M. Mogensen, Green 1 (2011) 141–169.
[3] N. Ortiz-Vitoriano, C. Bernuy-López, I. Ruiz de Larramendi, R. Knibbe, K. Thydén, A. Hauch, P. Holtappels, T. Rojo, Appl. Energy 104 (2013) 984–991.
[4] H. Schichlein, A.C. Müller, M. Voigts, A. Krügel, E. Ivers-Tiffée, J. Appl. Electrochem. 32 (2002) 875–882.
[5] N. Ortiz-Vitoriano, I. Ruiz de Larramendi, I. Gil de Muro, J.I. Ruiz de Larramendi, M.I. Arriortua, T. Rojo, Mater. Res. Bull. 45 (2010) 1513–1519.
[6] S.B. Adler, J.A. Lane, B.C.H. Steele, J. Electrochem. Soc. 143 (1996) 3554–3564.
[7] P. Hjalmarsson, M. Mogensen, J. Power Sources 196 (2011) 7237–7244.
[8] P. Holtappels, S. Duval, T. Graule, in: Proceedings of 8th European Solid Oxide Fuel cell Forum, 2008, pp. A0612–A0621.
[9] M.J. Jørgensen, M. Mogesen, J. Electrochem. Soc. 148 (2001) A433–A442.
[10] E.P. Murray, T. Tsai, S.A. Barnett, Solid State Ionics 110 (1998) 235–243.
[11] E. Siebert, A. Hammouche, M. Kleitz, Electrochim. Acta 40 (1995) 1741–1753.
[12] J. Misuzaki, H. Tagawa, K. Tsuneyoshi, A. Sawata, J. Electrochem. Soc. 138 (1991) 1867–1873.
[13] M.C. Brant, T. Matencio, L. Dessemond, R.Z. Domingues, Solid State Ionics 177 (2006) 915–921.
[14] R. Barford, M. Mogensen, T. Klemensø, A. Hagen, Y.L. Liu, P.V. Hendriksen, J. Electrochem. Soc. 154 (4) (2007) B371–B378.
[15] P. Holtappels, M.J. Jørgensen, S. Primhdal, M. Mogensen, C. Bagger, in: Proceedings of the 3rd European SOFC Forum, 1998, pp. 311–320.
[16] M. Balaguer, V.B. Vert, L. Navarrete, J.M. Serra, J. Power Sources 223 (2013) 214–220.
[17] J. Nielsen, T. Klemensø, P. Blennow, J. Power Sources 219 (2012) 305–316.
[18] H.J. Ko, J.-H. Myung, J.-H. Lee, S.-H. Hyun, J.S. Chung, Int. J. Hydrogen Energy 37 (2012) 17209–17216.
[19] S. McIntosh, S.B. Adler, J.M. Vohs, R.J. Gorte, Electrochem. Solid-State Lett. 7 (5) (2004) A111–A114.